A DEEP LEARNING FRAMEWORK FOR ROADS NETWORK DAMAGE ASSESSMENT USING POST-EARTHQUAKE LIDAR DATA

S.T. Seydi [1], H. Rastiveis [1,*]

[1] Dept. of Photogrammetry and Remote Sensing, School of Surveying and Geomatics Eng., University of Tehran, Tehran, Iran.
(seydi.teymoor, hrasti)@ut.ac.ir

Commission III, ICWG III/IVa

KEY WORDS: LiDAR Point Cloud, Earthquake, Deep learning, Conventional Neural Network, Roads damage map

ABSTRACT:

Roads network are the most important parts of urban infrastructures, which can cause difficulty to the city whenever they undergo a problem. This paper aims to provide and implement a deep learning-based method to determine the status of the streets network after an earthquake using LiDAR point cloud. The proposed framework composes of three main phases: (1) Deep features of LiDAR data are extracted using a Convolutional Neural Network (CNN). (2) The extracted features are used in a multilayer perceptron (MLP) neural network in which debris areas inside the road network are detected. (3) The amount of debris in each road is applied to damage index for classifying the road segments into blocked or un-blocked. To evaluate the efficiency of the proposed framework, LiDAR point cloud of the Port-au-Prince, Haiti after the 2010 Haiti earthquake was used. The overall accuracy of more than 97% proved the high performance of this framework for debris detection. Moreover, analyzing damage assessment of 37 road segments based on the detected debris and comparing to a visually generated damaged map, 31 of the road segments were correctly labelled as either blocked or un-blocked.

1. INTRODUCTION

Natural disasters, such as earthquakes, cause severe problems in people’s everyday life (Fan et al., 2019; Ferrentino et al., 2019). Earthquake is one of the most important disasters that frequently occurs all around the world (Chen et al., 2008; Ferrentino et al., 2018; Izadi et al., 2017; Moya et al., 2018). After an earthquake, it is crucial to know the status of the road network which plays a key role in disaster relief. Therefore, generating an accurate road network damage map, rapidly after earthquakes, which shows both blocked and un-blocked roads, is critical for rescue teams. In this case, due to the large coverage, agile and cost-effective properties of the Remote Sensing data such as LiDAR point clouds, they have become powerful data sources for mapping process (Seydi and Hasanlou, 2017). The damaged roads detection (DRD) can be defined as the process of separating the intact roads from blocked roads (Zheng et al., 2015). During the last decade, different damage detection methods using geospatial data such as LiDAR, high resolution optical dataset, syntactic aperture radar (SAR) have been developed (Fan et al., 2019; Izadi et al., 2017; Li et al., 2016; Rastiveis et al., 2015a).

These methods can be considered in two main categories: pixel-level, and object-level (Anniballe et al., 2018; Coulibaly et al., 2014; Kouchi and Yamazaki, 2005; Li et al., 2016). Pixel-level algorithms are fast and easy-to-implement which focus on extracting spatial and spectral features from the data in level of pixels. On the other hand, the object-level damage assessment methods are based on analysing a number of homogeneous segments (called image-objects) extracted from a segmentation technique (Rastiveis et al., 2018). They are usually time-consuming and complex due to the segmentation process. In this regard, Samadzadegan and Zarrinpanjeh, (2008) proposed an object-oriented method using pre- and post-event QuickBird images to detect damaged roads after the 2003 earthquake in Bam, Iran. They used spectral and spatial information for detecting shadows, objects, vegetation cover, and blocked roads. Auxiliary data such as pre-event vector map along the post-event WorldView II satellite images of the Haiti earthquake were used for DRD (Rastiveis et al., 2015). Izadi et al., (2017) extracted image objects using multi-resolution segmentation, and obtained a damage map using KNN classifier method based on texture features. They analysed the classification result in a Fuzzy system to detect un-block or blocked roads.

Although the abovementioned studies on DRD have shown promising results, they suffer many challenges such as the existence of shadow, noise, and atmospheric conditions, which may increase false alarm rate. This challenges are more seen in most of the change detection methods, specifically in the case of using traditional machine learning techniques. Also, performing the object-level classification is a time-consuming process, and the applied features for classification such as textural or spectral features are not robust. Generally, these DRD methods use multi-temporal dataset while the pre-event data may not be available for many places. To overcome these problems, this paper proposes a deep-leaning (DL) based framework for DRD using merely post-event LiDAR data.

LiDAR data provides accurate height information that facilitates the DRD purposes. This sort of data can be collected day or night time without the shadow problem caused by tall buildings (Axel and van Aardt, 2017). Moreover, the pre-processing of LiDAR data is simple compared to other RS datasets. Besides, using DL-based algorithms have recently become the fastest-growing trend in image processing (Ball et al., 2017; Heydari and Mountrakis, 2019; Ma et al., 2019). These algorithms have also shown excellent performance in many remote sensing applications such as classification, building extraction, and image registration (Ma et al., 2019; Wang et al., 2018; Wen et al., 2019). In this research, Convolutional Neural Network (CNN) which is one of the most suitable DL architectures for image classification is used for DRD. The aims of this study is to use deep features for DRD purposes, and evaluating their abilities in comparison with textural features for detecting debris area.

This paper is outlined as follows: Section 2 states the details of the proposed framework for DRD, and section 3 introduces study areas. The evaluation results of this study area are provided in section 4 the experimentation results are concluded in section 5.

2. PROPOSED FRAMEWORK FOR DRD

Figure 1 presents the structure of the proposed method. As can be seen from this figure, after pre-processing, the proposed method generates a streets road network damage map in three main steps of deep feature extraction, MLP classifier, and damage assessment. Each of which is described in the following subsections.

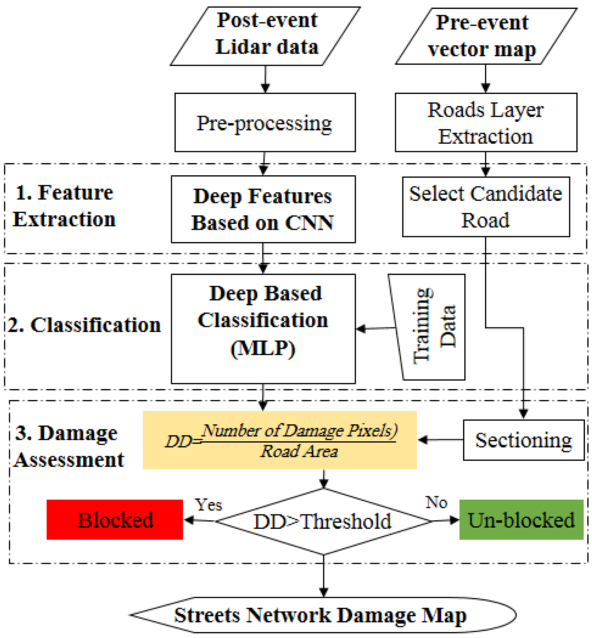

Figure 1. The proposed DL-based framework for damaged roads detection using LiDAR data.

2.1 Feature Extraction for DRD

Feature generation is one of the key steps in classification of RS data. The results of many classification algorithms have shown that adding spatial features along with spectral features improves the classification results (Rastiveis et al., 2015b). Therefore, features play a key role in the performance of data classification using machine learning techniques. For this end, this research investigates two groups of textural and DL-based features that have widely been used in RS data classification for DRD (Fan et al., 2019; Izadi et al., 2017; Li et al., 2016; Rastiveis et al., 2015a).

2.1.1 Textural Features

Texture information is a common descriptors for damage detection in Remote Sensing (Chen and Dou, 2018; Li et al., 2016), and can be defined as a piece of information based on the relation between the data of one pixel with its surrounding pixels in a window with a defined size. A texture feature may include descriptors such as density, equality, non-roughness, and size uniformity. These descriptors have been widely used to determine earthquake effects in the surface of roads using RS data. In this research, eight Haralick textures based on the co-occurrence matrix are used as the applied texture information. These texture features, which are mean, variance, homogeneity, contrast, dissimilarity, entropy, second moment, and correlation, have been selected due to their largely reported application in damage assessment in the literature (De Siqueira et al., 2013; Karathanassi et al., 2000; Zhang et al., 2017). More details about different textures can be found in (Karathanassi et al., 2000; Zucker and Terzopoulos, 1980).

2.1.2 DL-based Features

DL-based methods could automatically learn informative representations of input data with multiple levels of abstraction (Ball et al., 2017). A DL framework can be seen in four main different architectures of CNN, deep belief networks (DBNs), recurrent NN (RNN), and auto-encoder (AE) (Ball et al., 2017). The CNN uses stacked convolutional kernels to learn the features of images, so both of the spectral and the textural information in spatial space are learned (Zhao et al., 2018). A CNN-based classification method generally consists two main parts of feature extractor and a soft max that usually used an MLP that assigns class labels (Yang and Cervone, 2019). It can be created based on connections between the input data and the output labels to obtain the classification results (Ma et al., 2019; Wen et al., 2019). Deep features in CNN can be extracted through multiple layers of operation: convolution layers, pooling layer, nonlinear activation functions, and normalization (Heydari and Mountrakis, 2019). In which, after training, for each pixel a 28×28 patch is considered as input data. Then through two convolution layers considering 3×3 kernels the deep features are extracted to be used in the classification. Figure 2 represents the architecture of the implemented CNN for extracting deep features in this research.

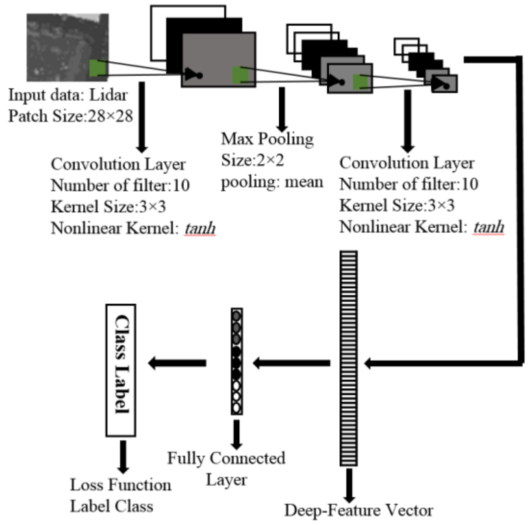

Figure 2. The architecture of the applied CNN for extracting deep features

2.2 Classification

In automated DRD using RS data, either textural features or deep features are fed to a classifier to detect the class label. Due to the fact that in DRD, debris areas on the streets should

https://doi.org/10.5194/isprs-archives-XLII-4-W18-955-2019 | © Authors 2019. CC BY 4.0 License.

be accurately detected, the main purpose of classification is detection and discrimination of the debris areas on the roads surface from other classes. Inside a road area in a LiDAR data, four classes of cars, intact roads, debris, and trees are considered. In this section, two classification methods of Support Network Machines (SVM) and Artificial Neural Network (ANN) which have been frequently used in damage analysis are described.

2.2.1 SVM classifier

SVM classifier has widely been used in classification of optical high resolution RS data for urban areas. It is a supervised machine learning algorithm which is commonly used for classification purposes, and is based on the statistical learning theory (Cortes and Vapnik, 1995). The main idea behind SVM is to find a hyperplane that maximizes the margin between the two classes (Cortes and Vapnik, 1995). This algorithm has several critical parameters including kernel parameters and the penalty coefficient (C). This research used radial basis function (RBF) as kernel in the implemented SVM. One can refer to (Bishop, 2006; Chen, 2015) for more details of SVM classifier.

2.2.2 ANN classifier

ANN has also been used in a number of RS data classification research. A simple ANN architecture sually has an input layer, hidden layer and output layer. This architecture is called Multi-Layer Perceptron (MLP) because of the multiple layer. In MLP classifier, the main idea for learning is adjusting the weights in the node to minimize the difference between the output node activation and the output (Bishop, 2006; Chen, 2015; Zhang et al., 2019). In MLP the standard back-propagation is used for supervised learning (Zhang et al., 2019; Zhang et al., 2018), in which the error is back-propagated through the network, and weight adjustment is made using a recursive method. This process continues until the error became lower than a desired value. The MLP classifier has many parameters that need to be tuned including number of hidden layers, activation function, learning rate, momentum rate, and maximum number of iterations,. More details of MLP algorithm can be studied in (Bishop, 2006; Chen, 2015).

2.3 Damage Assessment

The estimation of damage degree of each road is the main goal of this step, which can be performed through various methods. Wang et al., (2015) investigated the indicators of road damage assessment based on road width, length, area, and relative parameters of damaged road. They showed that the damage assessment based on width parameter has best performance. So, this research used width parameter as a criterion for damage assessment. In this research, each road is firstly divided into a number of tiles along the road, and the largest debris polygon inside each section is used to determine whether or not the section is block. In which, the Damage Degree (DD) of each section can be defined as the relation between the width of the largest debris polygon (W_L) to the road width (W_R) as follows:

$$DD=\frac{W_L}{W_R}. \qquad (1)$$

Then the un-blocked or blocked section roads are determined based on their damage degree and a suitable threshold, which may be specified as predefined knowledge. Final decision about the situation of each road can be made based on the number of blocked sections in the road.

3. DATASET AND CASE STUDY

The proposed method was evaluated using the LiDAR raster data of the Port-au-Prince, Haiti acquired after the 2010 earthquake and with 1 m spatial resolution. Within these data set, a study area of 592×555 (m^2) region including 37 roads was selected. Also, the 1:2000 vector map of this area was applied as an ancillary data. Figure 3 shows the LiDAR raster data and the vector map of the case study which were used in this study.

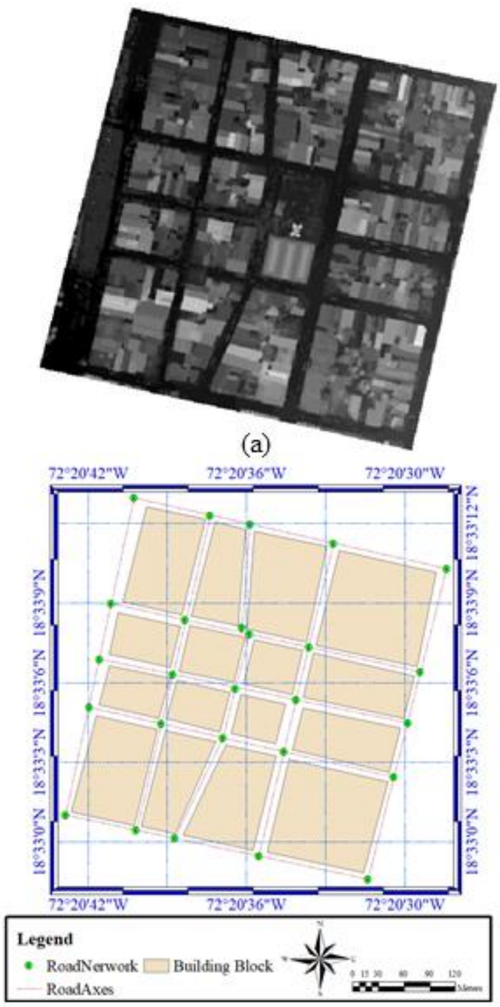

Figure 3. (a) Selected test area for evaluation of the proposed method. (a) The post-event LiDAR raster data (b) The roads network layer from the pre-event vector map.

4. EXPRIMENTS AND DISCUSSION

4.1 Results

Before executing the DRD process based on the proposed algorithm, the data pre-processing is performed to obtain more reliable results. In this regard, the LiDAR raster data is co-registred with vector data. After applying the pre-processing steps, all the objects outside streets network were masked from LiDAR raster data by overlaying the extracted roads network from vector map. However, in the classification process all the entire image including non-road pixels in the neighborhood of the road pixels are used during the feature extraction.

Two groups of textural and deep features were extracted from the raster data. In the first group, 8 textural features of mean, variance, homogeneity, contrast, dissimilarity, entropy, second moment, and correlation were extracted by considering a 3×3 kernel. Next group features are the deep features that extracted by CNN algorithm according to the architecture shown in Figure 2. The optimal parameters of CNN are: batch size is 28×28, the size kernel of convolution in the first layer is 3×3, third layer is 3×3, the size of kernel for pooling layer is 2×2, the type of pooling is mean pooling, number of epochs is 15, and number of filters in first and second layers is 10. Various types of nonlinear activation functions such as ReLU, tanh, and sigmoid were tested that the hyperbolic tangent (tanh) activation function was more fit to the LiDAR data based on defined architecture in the CNN network. The training dataset were extracted in four main classes including Car, Tree, Debris, Intact Road. Figure 4 presents a number of sample patch that were used in training process.

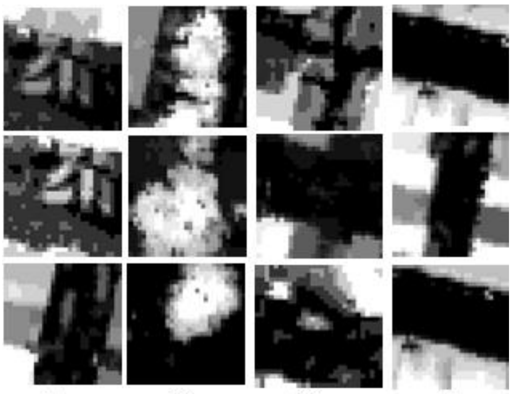

(a) (b) (c) (d)

Figure 4. Sample of training data, (a) car, (b) tree, (c) debris, and (d) intact road

In this research, the classification were performed in two different strategies and the results were analysed ether visually or numerically. First, classification of the LiDAR data based on textural features through the MLP and the SVM classifiers. The other strategy was the MLP classifier using the extracted CNN-based deep features. The optimum value of the penalty coefficient (C) parameter in SVM was considered 2^5, and kernel parameter, gamma (γ), is 2^{-11}. The parameters of the MLP classifier are as follows: number of hidden layer is 5, number of iteration is 100, training momentum is 0.1, and training rate is 0.001. Moreover, in order to make a fair comparison between different strategies, the size of training data was equally considered in all cases. Here, totally 4553 sample pixels for 4 classes were manually collected, which 67% and 33% considered as training and test data, respectively. Figure 5 presents the classification results obtained in these strategies.

Based on the presented results, textural information in both classifiers in the case of using textural information miss-detected some of the classes, specifically the Car class, which were classified as debris. Also, there are many pixels false detected as debris pixels by texture information, while this theme is low in result of deep features. Conversely, as can be seen from Figure 5-c, the MLP classifier based on deep features provided more promising results, and all classes were successfully detected. The classification results were also evaluated based on the confusion matrix. Using this matrix, conventional measures including Overall Accuracy, Omission Error, Commission Error, User Accuracy, and Producer Accuracy were calculated.

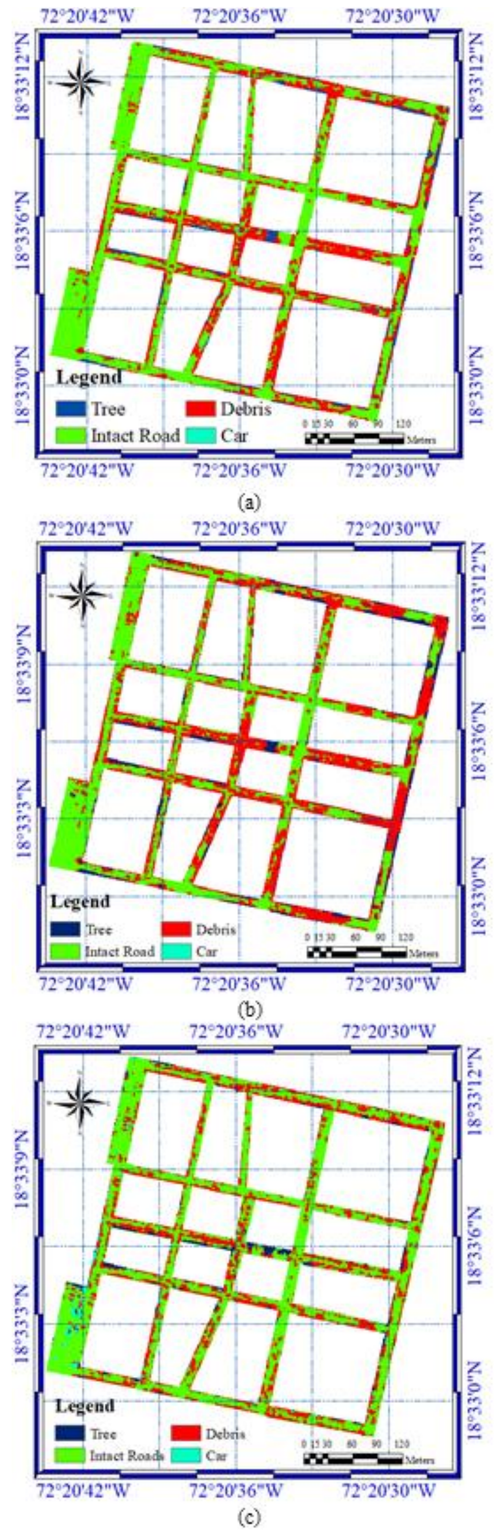

Figure 5. The result of classification on LiDAR data: (a) The MLP classifier using textural features; (b) The SVM classifier using textural features; (c) The MLP classifier applying extracted deep features by the CNN.

https://doi.org/10.5194/isprs-archives-XLII-4-W18-955-2019 | © Authors 2019. CC BY 4.0 License.

The obtained confusion matrices are presented in Table 1, and the numerical results of the classifications are summarized in Table 2. As shown in these tables, the classification based on LiDAR data could present acceptable results. In which, all classifiers have presented accuracy of more than 90%. Also, the numerical analysis confirms the superiority of the MLP classifier based on deep features in comparison with other strategies. It is evident that the CNN-based classification has detected more car pixels in comparison with the other classifiers based on textural information. Moreover, the lowest omission and commission errors for all four classes also belong to this classification.

		Reference				Overall Accuracy %	Classification Error (%)
		Tree	Intact Road	Debris	Car		
MLP-TF	Tree	289	0	26	4	89.4	10.6
	Intact Road	0	641	34	1		
	Debris	20	25	407	47		
	Car	1	0	1	3		
SVM-TF	Tree	287	0	17	8	89.9	10.1
	Intact Road	0	640	30	1		
	Debris	23	26	420	45		
	Car	0	0	1	1		
MLP-CNN	Tree	308	0	0	0	**97.7**	**2.3**
	Intact Road	0	663	16	0		
	Debris	2	3	452	13		
	Car	0	0	1	42		

Table 1. Confusion Matrices of the classification results for different strategies.

	MLP-TF				SVM-TF				MLP-CNN			
	User Accuracy	Commission Error	Omission error	Producer Accuracy	User Accuracy	Commission Error	Omission error	Producer Accuracy	User Accuracy	Commission Error	Omission error	Producer Accuracy
Tree	90.6	9.4	6.8	93.2	92.0	8	7.4	82.6	**100**	**0**	**0.6**	**99.4**
Intact Road	94.8	5.2	3.8	96.2	95.4	4.6	3.9	96.1	**97.6**	**2.4**	**0.5**	**99.5**
Debris	81.6	18.4	13	87	81.7	18.3	10.3	89.7	**96.2**	**3.8**	**3.6**	**96.4**
Car	60	40	94.5	5.5	50	50	98.2	1.8	**97.7**	**2.3**	**23.4**	**76.4**

Table 2. Summary of the numerical evaluation of the classification strategies based on the obtained confusion matrices in Table 1.

The final phase of DRD is the analysis of debris areas for determining the situation of the roads. Here, due to the excellent performance of MLP-CNN, the classified map of this strategy was selected for damage assessment. Each road was firstly divided into different sections with 1-meter space along the road. Here, due to existence of left and right side walks, a buffer space equal to 15% of each road width from the roads were ignored. After calculating the DD index for each section, 0.6 was considered as the threshold for detecting the sections situation. In which, if the DD value for a section is lower than 0.6, that section would labelled as un-blocked section. Otherwise, the section is labelled as blocked section. Note, this threshold is defined as predefined parameters. Eventually, if 10% of tiles are blocked, the road would be labelled blocked. Figure 7 presents the obtained final damage map for the roads network of the test area displaying two classes of un-blocked and blocked roads. Based on this figure, among 37 road segments in the study area, 31 of them were successfully labelled, and only 6 streets were labelled mistakenly.

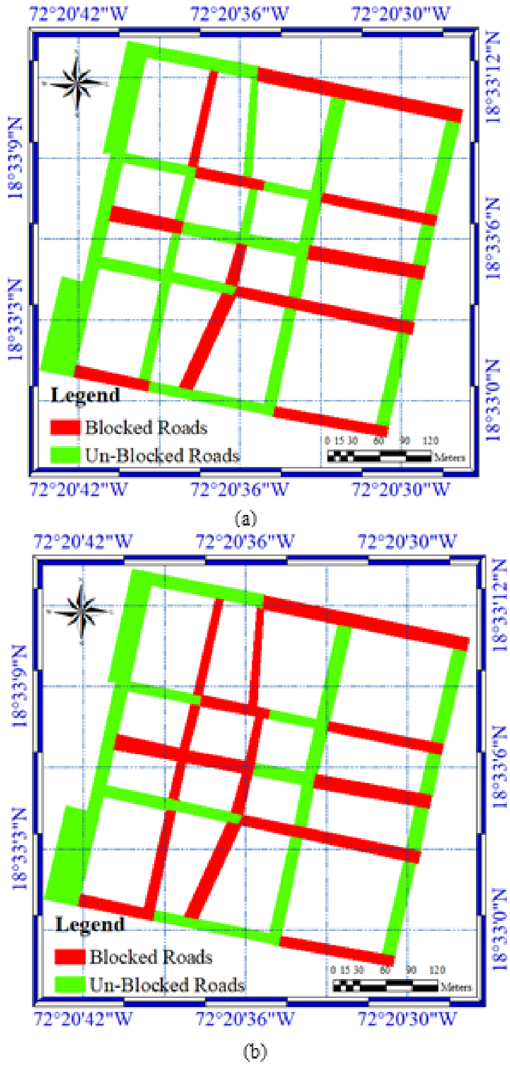

Figure 7. The result of DRD for the test area using the proposed framework. (a) The resulted map using the MLP-CNN classification; (b) Ground truth.

4.2 Discussion

This research presented an efficient and robust framework for DRD based on post-event LiDAR data. The proposed framework were tested using the Haiti dataset. Two groups of textural features and deep features were investigated for classification of LiDAR data. One of the most issues in the performance of DRD process is detecting debris areas on the roads which cause blockage. Therefore, the result of DRD has absolute dependency on the accuracy of the classification. The results of classification based on deep features had a superior advantage compared to textural features. However, the MLP classifier based on deep features includes a number of hyper-parameters which need to be carefully set. This is one of the most common challenges in deep learning algorithms. Moreover, determining the optimal architecture, and optimally training are other challenges of this method. Although these challenges have been seen among deep learning systems, the presented results showed that it is treasured, and deep features showed excellent results in comparison to textural features in DRD. Rastiveis et al., (2015b) proposed a framework that used texture features based on SVM and ANN classifier that presented acceptable results, but the proposed framework in this paper has higher accuracy in comparison to that framework. Another advantage of this method is that in our proposed method merely post-event LiDAR data is applied while in that method optical RS data in addition to LiDAR data is needed.

5. CONCLUSION

This paper presented a deep learning framework for DRD based on post-event LiDAR data plus a pre-event vector roads network as an ancillary data. Two groups of features using three classification algorithms were investigated to classify the roads pixels into four classes. The first group features were Haralick textural features including mean, variance, homogeneity, contrast, dissimilarity, entropy, second moment, and correlation that extracted by co-occurrence matrix. The classifier algorithms for this group were SVM and MLP based on feed forward. The second group feature was deep features that obtained by CNN algorithm which imported to the MLP classifier. The classification results were analysed both visually and numerically, and MLP classifier with CNN-based deep features reported more than 97% accuracy that was the highest rate among all the cases. Using this classification results, 31 streets out of 37 roads were correctly labelled by this DRD framework.

Generally, using deep features due to their excellent performance are robust features which can be used for DRD purposes. Moreover, it can be used instead of the traditional features such as textural or spectral features. Although, in this research, promising results were obtained based on LiDAR data, however, using other remote sensing data such as optical high resolution could improve the results.

REFERENCES

Anniballe, R., Noto, F., Scalia, T., Bignami, C., Stramondo, S., Chini, M., Pierdicca, N., 2018. Earthquake damage mapping: An overall assessment of ground surveys and VHR image change detection after L'Aquila 2009 earthquake. *Remote Sensing of Environment* 210, 166-178.

Axel, C., van Aardt, J., 2017. Building damage assessment using airborne lidar. *Journal of Applied Remote Sensing* 11, 046024.

Ball, J.E., Anderson, D.T., Chan, C.S., 2017. Comprehensive survey of deep learning in remote sensing: theories, tools, and challenges for the community. *Journal of Applied Remote Sensing* 11, 042609.

Bishop, C.M., 2006. Pattern recognition and machine learning. *Springer*.

Chen, C.-h., 2015. Handbook of pattern recognition and computer vision. *World Scientific.*

Chen, S.-r., Ma, H.-j., Fan, Y.-d., XU, F., LIAN, J., 2008. Road damage assessment from high resolution satellite remote sensing imagery in Wenchuan Earthquake. *Journal of remote sensing* 6.

Chen, Z., Dou, A., 2018. Road Damage Extraction From Post-Earthquake Uav Images Assisted By Vector Data. *International Archives of the Photogrammetry, Remote Sensing & Spatial Information Sciences* 42.

Cortes, C., Vapnik, V., 1995. Support-vector networks. *Machine learning* 20, 273-297.

Coulibaly, I., Spiric, N., Sghaier, M.O., Manzo-Vargas, W., Lepage, R., St-Jacques, M., 2014. Road extraction from high resolution remote sensing image using multiresolution in case of major disaster, 2014 *IEEE Geoscience and Remote Sensing Symposium.* IEEE, pp. 2712-2715.

De Siqueira, F.R., Schwartz, W.R., Pedrini, H., 2013. Multi-scale gray level co-occurrence matrices for texture description. *Neurocomputing* 120, 336-345.

Fan, X., Nie, G., Deng, Y., An, J., Zhou, J., Li, H., 2019. Rapid detection of earthquake damage areas using VIIRS nearly constant contrast night-time light data. *International Journal of Remote Sensing* 40, 2386-2409.

Ferrentino, E., Marino, A., Nunziata, F., Migliaccio, M., 2019. A dual–polarimetric approach to earthquake damage assessment. *International Journal of Remote Sensing* 40, 197-217.

Ferrentino, E., Nunziata, F., Migliaccio, M., Vicari, A., 2018. A sensitivity analysis of dual-polarization features to damage due to the 2016 Central-Italy earthquake. *International journal of remote sensing* 39, 6846-6863.

Heydari, S.S., Mountrakis, G., 2019. Meta-analysis of deep neural networks in remote sensing: A comparative study of mono-temporal classification to support vector machines. *ISPRS Journal of Photogrammetry and Remote Sensing* 152, 192-210.

Izadi, M., Mohammadzadeh, A., Haghighattalab, A., 2017. A new neuro-fuzzy approach for post-earthquake road damage assessment using GA and SVM classification from QuickBird satellite images. *Journal of the Indian Society of Remote Sensing* 45, 965-977.

Karathanassi, V., Iossifidis, C., Rokos, D., 2000. A texture-based classification method for classifying built areas according to their density. *International Journal of Remote Sensing* 21, 1807-1823.

Kouchi, K., Yamazaki, F., 2005. Damage detection based on object-based segmentation and classification from high-resolution satellite images for the 2003 Boumerdes, Algeria earthquake, *Proceedings of the 26th Asian conference on Remote Sensing*, Hanoi, Vietnam.

Li, Q., Zhang, J., Wang, N., 2016. Damaged road extraction from post-seismic remote sensing images based on gis and

This contribution has been peer-reviewed.
https://doi.org/10.5194/isprs-archives-XLII-4-W18-955-2019

object-oriented method, *IEEE International Geoscience and Remote Sensing Symposium (IGARSS)*. IEEE, pp. 4247-4250.

Ma, L., Liu, Y., Zhang, X., Ye, Y., Yin, G., Johnson, B.A., 2019. Deep learning in remote sensing applications: A meta-analysis and review. *ISPRS Journal of Photogrammetry and Remote Sensing* 152, 166-177.

Moya, L., Yamazaki, F., Liu, W., Yamada, M., 2018. Detection of collapsed buildings from lidar data due to the 2016 Kumamoto earthquake in Japan. *Natural Hazards and Earth System Sciences* 18, 65.

Rastiveis, H., Eslamizade, F., Hosseini-Zirdoo, E., 2015a. Building Damage Assessment After Earthquake Using Post-Event Lidar Data. *International Archives of the Photogrammetry, Remote Sensing & Spatial Information Sciences* 40.

Rastiveis, H., Hosseini-Zirdoo, E., Eslamizade, F., 2015b. Automatic Blocked Roads Assessment After Earthquake Using High Resolution Satellite Imagery. *International Archives of the Photogrammetry, Remote Sensing & Spatial Information Sciences* 40.

Rastiveis, H., Khodaverdi zahraee, N., Jouybari, A., 2018. Object-Oriented Classification Of Lidar Data For Post-Earthquake Damage DetectioN. *International Archives of the Photogrammetry, Remote Sensing & Spatial Information Sciences* XLII-3/W4, 421-427.

Samadzadegan, F., Zarrinpanjeh, N., 2008. Earthquake destruction assessment of urban roads network using satellite imagery and fuzzy inference systems. *The international archives of the photogrammetry, remote sensing and spatial information sciences* 37, 409-414.

Seydi, S.T., Hasanlou, M., 2017. A new land-cover match-based change detection for hyperspectral imagery. *European Journal of Remote Sensing* 50, 517-533.

Wang, J., Qin, Q., Zhao, J., Ye, X., Feng, X., Qin, X., Yang, X., 2015. Knowledge-Based Detection and Assessment of Damaged Roads Using Post-Disaster High-Resolution Remote Sensing Image. *Remote Sensing* 7, 4948-4967.

Wang, S., Quan, D., Liang, X., Ning, M., Guo, Y., Jiao, L., 2018. A deep learning framework for remote sensing image registration. *ISPRS Journal of Photogrammetry and Remote Sensing* 145, 148-164.

Wen, C., Sun, X., Li, J., Wang, C., Guo, Y., Habib, A., 2019. A deep learning framework for road marking extraction, classification and completion from mobile laser scanning point clouds. *ISPRS Journal of Photogrammetry and Remote Sensing* 147, 178-192.

Yang, L., Cervone, G., 2019. Analysis of remote sensing imagery for disaster assessment using deep learning: a case study of flooding event. *Soft Computing*, 1-16.

Zhang, A., Sun, G., Ma, P., Jia, X., Ren, J., Huang, H., Zhang, X., 2019. Coastal Wetland Mapping with Sentinel-2 MSI Imagery Based on Gravitational Optimized Multilayer Perceptron and Morphological Attribute Profiles. *Remote Sensing* 11, 952.

Zhang, C., Pan, X., Li, H., Gardiner, A., Sargent, I., Hare, J., Atkinson, P.M., 2018. A hybrid MLP-CNN classifier for very fine resolution remotely sensed image classification. *ISPRS Journal of Photogrammetry and Remote Sensing* 140, 133-144.

Zhang, X., Cui, J., Wang, W., Lin, C., 2017. A study for texture feature extraction of high-resolution satellite images based on a direction measure and gray level co-occurrence matrix fusion algorithm. *Sensors* 17, 1474.

Zhao, X., Gao, L., Chen, Z., Zhang, B., Liao, W., 2018. CNN-based Large Scale Landsat Image Classification, *Asia-Pacific Signal and Information Processing Association Annual Summit and Conference (APSIPA ASC). IEEE*, pp. 611-617.

Zheng, Z., Pu, C., Zhu, M., Xia, J., Zhang, X., Liu, Y., Li, J., 2015. Damaged road extracting with high-resolution aerial image of post-earthquake, *International Conference on Intelligent Earth Observing and Applications*, *International Society for Optics and Photonics*, p. 980807.

Zucker, S.W., Terzopoulos, D., 1980. Finding structure in co-occurrence matrices for texture analysis. *Computer graphics and image processing* 12, 286-308.